Langmuir
Article
pubs.acs.org/Langmuir

Schizophrenic Behavior of a Thermoresponsive Double Hydrophilic Diblock Copolymer at the Air−Water Interface

Rute I. S. Romão,[†] Mariana Beija,[‡,§] Marie-Thérèse Charreyre,[§,∥] José Paulo S. Farinha,[‡] Amélia M. P. S. Gonçalves da Silva,*[,†] and José M. G. Martinho*[,‡]

[†]*Centro de Química Estrutural, and* [‡]*Centro de Química-Física Molecular and IN − Institute of Nanosciences and Nanotechnology, Instituto Superior Técnico, Universidade Técnica de Lisboa, 1049-001 Lisboa, Portugal, and* [§]*Unité Mixte CNRS-bioMérieux, ENS de Lyon, 46 allée d'Italie, 69364 Lyon Cedex 07, France.* [∥]*Current address: Laboratoire Joliot-Curie and Laboratoire Ingénierie des Matériaux Polymères, ENS de Lyon, 46 allée d'Italie, 69364 Lyon Cedex 07, France.*

Received July 10, 2009. Revised Manuscript Received September 1, 2009

The thermoresponsive behavior of the rhodamine B end-labeled double hydrophilic block copolymer (DHBC) poly(*N*,*N*-dimethylacrylamide)-*b*-poly(*N*,*N*-diethylacrylamide) (RhB-PDMA$_{207}$-*b*-PDEA$_{177}$) and the 1:1 segmental mixture of PDEA and rhodamine B end-labeled PDMA homopolymers was studied over the range of 10−40 °C at the air−water interface. The increase in collapse surface pressure (second plateau regime) of the DHBC with temperature confirms the thermoresponsiveness of PDEA at the interface. The sum of the $\pi-A$ isotherms of the two single homopolymers weighted by composition closely follows the $\pi-A$ isotherm of the DHBC, suggesting that the behavior of each block of the DHBC is not influenced by the presence of the other block. Langmuir−Blodgett monolayers of DHBC deposited on glass substrates were analyzed by laser scanning confocal fluorescence microscopy (LSCFM), showing schizophrenic behavior: at low temperature, the RhB-PDMA block dominates the inside of bright (core) microdomains, switching to the outside (shell) at temperatures above the lower critical solution temperature (LCST) of PDEA. This core−shell inversion triggered by the temperature increase was not detected in the homopolymer mixture. The present results suggest that both the covalent bond between the two blocks of the DHBC and the tendency of rhodamine B to aggregate play a role in the formation of the bright cores at low temperature whereas PDEA thermoaggregation is responsible for the formation of the dark cores above the LCST of PDEA.

Introduction

Stimuli-responsive copolymers have attracted considerable attention from the scientific community by virtue of their potential in biotechnology, medicine, pharmaceutics, and bioengineering.[1−4] Double-hydrophilic block copolymers (DHBCs) combining two different hydrophilic blocks may form random aggregates, micelles, or even more organized structures such as liposomes in aqueous media.[5−11] This kind of aggregation can be created or destroyed by an external stimulus if one of the DHBC blocks is stimuli-responsive. External stimuli in an aqueous medium may render this block insoluble whereas the copolymer remains in solution because of the hydrophilic character of the other block. The study of DHBCs at interfaces is of the utmost importance because of their possible use in drug delivery and biomedical applications.[12−14]

By increasing the temperature above their lower critical solution temperature (LCST), thermoresponsive polymers undergo a phase separation in which a polymer-rich phase separates and eventually precipitates from a solvent-rich phase. *N*-Alkyl-substituted polyacrylamides are generally thermoresponsive in water, with poly(*N*-isopropylacrylamide) (PNIPAM) being the most studied because it has a phase transition at 32 °C, which is close to physiological temperature.[15,16] This entropically driven transition results from the release of the structured hydrogen-bonded water from the amide groups and the consequent increase in the hydrophobic interactions between the isopropyl groups.[15] This leads to the collapse of PNIPAM coils into globules (coil−globule transition),[17,18] which further associate to form larger aggregates that eventually precipitate.

Another thermoresponsive polymer, poly(*N*,*N*-diethylacrylamide) (PDEA), has been receiving increasing attention lately because it is biocompatible and, in spite of the absence of amide protons, has an LCST around physiological temperature (31−34 °C).[19−21] At temperatures below the LCST, the ethyl groups

*Corresponding authors. E-mail: ameliags@ist.utl.pt; jgmartinho@ist.utl.pt.

(1) Liu, S.; Maheshwari, R.; Kiick, K. *Macromolecules* **2009**, *42*, 3–13.
(2) York, A. W.; Kirkland, S. E.; McCormick, C. L. *Adv. Drug Delivery Rev.* **2008**, *60*, 1018–1036.
(3) Kumar, A.; Srivastava, A.; Galaev, I. Y.; Mattiasson, B. *Prog. Polym. Sci.* **2007**, *32*, 1205–1237.
(4) Rzaev, Z. M. O.; Dinçer, S.; Piskin, E. *Prog. Polym. Sci.* **2007**, *32*, 534–595.
(5) Arotçarena, M.; Heise, B.; Ishaya, S.; Laschewsky, A. *J. Am. Chem. Soc.* **2002**, *124*, 3787–3793.
(6) Maeda, Y.; Mochiduki, H.; Ikeda, I. *Macromol. Rapid Commun.* **2004**, *25*, 1330–1334.
(7) Dai, S.; Ravi, P.; Tam, K. C.; Mao, B. W.; Gan, L. H. *Langmuir* **2003**, *19*, 5175–5177.
(8) Nuopponen, M.; Ojala, J.; Tenhu, H. *Polymer* **2004**, *45*, 3643–3650.
(9) Cai, Y.; Armes, S. P. *Macromolecules* **2004**, *37*, 7116–7122.
(10) Rao, J.; Luo, Z.; Ge, Z.; Liu, H.; Liu, S. *Biomacromolecules* **2007**, *8*, 3871–3878.
(11) Zang, X.; Li, J.; Li, W.; Zhang, A. *Biomacromolecules* **2007**, *8*, 3557–3567.
(12) Xu, J.; Liu, S. *Soft Matter* **2008**, *4*, 1745–1749.
(13) Cheng, C.; Wei, H.; Shi, B.-X.; Cheng, H.; Li, C.; Gu, Z.-W.; Cheng, S.-X.; Zhang, X.-Z.; Zhuo, R.-X. *Biomaterials* **2008**, *29*, 497–505.
(14) Agut, W.; Brûlet, A.; Taton, D.; Lecommandoux, S. *Langmuir* **2007**, *23*, 11526–11533.
(15) Schild, H. G. *Prog. Polym. Sci.* **1992**, *17*, 163–249.
(16) Pelton, R. *Adv. Colloid Interface Sci.* **2008**, *85*, 1–33.
(17) Wang, X.; Qiu, X.; Wu, C. *Macromolecules* **1998**, *31*, 2972–2976.
(18) Kujawa, P.; Aseyev, V.; Tenhu, H.; Winnik, F. *Macromolecules* **2006**, *39*, 7686–7693.
(19) Ding, Z.; Fong, R. B.; Long, C. J.; Stayton, P. S.; Hoffman, A. S. *Nature* **2001**, *411*, 59–62.
(20) Hiratani, H.; Alvarez-Lorenzo, C. *J. Controlled Release* **2002**, *83*, 223–230. Hiratani, H.; Alvarez-Lorenzo, C. *Biomaterials* **2004**, *25*, 1105–1113.
(21) Valuev, L. I.; Valuev, I. L.; Shanazarova, I. M. *Appl. Biochem. Microbiol.* **2006**, *42*, 27–30.

are hydrated and most of the C=O groups of PDEA are hydrogen bonded with one or two water molecules. By increasing the temperature above the phase transition, most of the ethyl groups become dehydrated and associate through hydrophobic interactions, whereas the C=O groups continue to be hydrated in spite of the decrease in hydrogen bonding.[22] The transition is driven by the increase in entropy resulting from the release of the water molecules that surround the ethyl groups and the consequent increase in hydrophobic interactions.

The molecular design of thermoresponsive polymers, concerning their molecular structure and functional groups, is crucial for the creation of specific smart biomaterials and biointerfaces.[23,24] The air−water interfacial behavior of amphiphilic copolymers can be studied by using the Langmuir technique.[25] In particular, combining the Langmuir and the Langmuir−Blodgett (LB) techniques, the conformational changes undergone by the thermoresponsive copolymers around the LCST can be followed and further characterized by specific and powerful techniques of surface characterization, namely, AFM, neutron reflectivity and scattering, electron microscopy, FTIR, and XPS.[26,27]

The thermoresponsive behavior of PDEA and of the amphiphilic poly(*N*-decylacrylamide)-*b*-poly(*N*,*N*-diethylacrylamide) block copolymer ($PDcA_{11}$-*b*-$PDEA_{231}$) composed of a short hydrophobic block of PDcA and a long block of PDEA was studied at the air−water interface between 10 and 40 °C.[28] The low and nearly flat morphology of LB monolayers of PDEA suggested the formation of (2D) aggregates with low cohesion whereas $PDcA_{11}$-*b*-$PDEA_{231}$ was found to form globular and higher (3D) aggregates with extra cohesion introduced by the hydrophobic block.[28]

In this work, we study the thermoresponsive behavior of a double hydrophilic block copolymer (DHBC) composed of a PDEA block covalently linked to a rhodamine B end-labeled poly(*N*,*N*-dimethylacrylamide) (PDMA) block (RhB-$PDMA_{207}$-*b*-$PDEA_{177}$) and the mixture of PDEA and RhB-PDMA homopolymers at the air−water interface. The presence of rhodamine B at the end of the PDMA chain allowed us to characterize further the film organization and distribution of aggregates in LB monolayers transferred at several temperatures and surface pressures by laser scanning confocal fluorescence microscopy (LSCFM) of the supported polymer films.[29] This study revealed a core−shell inversion, the so-called schizophrenic behavior, triggered by the temperature increase: at low temperature, the RhB-PDMA block dominates the inside of bright (core) microdomains, switching to the outside (shell) at temperatures above the LCST of PDEA. The schizophrenic behavior of stimuli-responsive copolymers has been reported in aqueous solution.[5,6,9,11,30] As far as we are aware, the present work is the first reporting the schizophrenic behavior of a thermoresponsive polymer at the air−water interface.

Experimental Section

Materials. *N*,*N*-Diethylacrylamide (DEA) was purchased from Monomer-Polymer & Dajac Laboratories, and *N*,*N*-dimethylacrylamide (DMA) was obtained from Aldrich (both with a purity >99%). Both monomers were purified by distillation under reduced pressure to remove inhibitor. DEA was distilled at 26 °C and 0.2 mbar in the presence of 4-methoxyphenol, and DMA was distilled at 24 °C and 0.4 mbar in the presence of hydroquinone. The initiator, 2,2′-azobis(isobutyronitrile) (AIBN) (Fluka, 98%), was purified by recrystallization from ethanol. Dimethylsulfoxide (DMSO) (Aldrich, anhydrous, 99.9%), dimethylformamide (DMF) (Fluka, 99.9%), acetone-d_6 (SDS), dimethylsulfoxide-d_6 (Aldrich 99.96%), lithium bromide (Merck), and trioxane (Acros, 99%) were used as received.

Poly(*N*,*N*-diethylacrylamide) (PDEA). The synthesis of the PDEA sample has been described elsewhere.[28]

RhB-poly(*N*,*N*-dimethylacrylamide) (RhB-PDMA). The rhodamine B-labeled PDMA homopolymer (RhB-PDMA) was obtained from the RAFT polymerization of DMA using a rhodamine B-modified dithiobenzoate as a chain-transfer agent (RhB-CTA).[31] DMA (0.77 g, 7.8 mmol), RhB-CTA (19.4 mg, 25.7 μmol), AIBN (0.8 mg, 2.74 μmol), DMSO (4.7 mL), and trioxane (0.05 g, 0.06 mmol, the ^{1}H NMR internal reference) were introduced into a Schlenk tube equipped with a magnetic stirrer. The mixture was degassed by five freeze−evacuate−thaw cycles and then heated under nitrogen in a thermostatted oil bath (75 °C). Periodically, aliquots of the polymerization medium were withdrawn to determine the monomer conversion by ^{1}H NMR. Typically, 400 μL of acetone-d_6 was added to 200 μL of each sample, and the NMR spectrum was recorded using a Bruker AC 200 spectrometer (200 MHz). Monomer consumption was determined from the area of vinylic protons using trioxane (5.1 ppm) as the internal reference. The final polymer (obtained at 39% conversion) was diluted 10-fold in Millipore H_2O, purified by dialysis at 4 °C for 5 days using a dialysis cassette (Slide-A-Lyzer) from Pierce with a cutoff (MWCO) of 3500 Da, and finally freeze dried to yield a fluffy pink compound.

RhB-poly(*N*,*N*-dimethylacrylamide)-*block*-poly(*N*,*N*-diethylacrylamide) (RhB-$PDMA_{207}$-*b*-$PDEA_{177}$). The block copolymer with the molecular structure shown in Chart 1 was synthesized by sequential reversible addition−fragmentation chain-transfer (RAFT) polymerization. A rhodamine B-labeled PDMA polymer sample was used as a macro-CTA in the RAFT polymerization of DEA in DMSO-d_6 ([DEA] = 1.0 mol L^{-1}) at 90 °C under nitrogen using AIBN as an initiator. The final block copolymer (obtained at 42% conversion) was purified by dialysis at 4 °C for 5 days using a dialysis cassette (Slide-A-Lyzer) from Pierce with a MWCO of 3500 Da and finally freeze dried to yield a fluffy pink solid.

Polymer Characterization. The number-average molecular weight (M_n) and polydispersity index (M_w/M_n) of the polymer samples were determined by size-exclusion chromatography (SEC) using a solution of 0.05 M LiBr in DMF as the eluent with a flow rate of 0.3 mL min^{-1} at 30 °C, three Phenogel columns (10^4, 10^3, and 10^2 Å, 5 μm, 7.8 × 300 mm) connected in series and calibrated with narrow PDMA samples, a Waters 2410 refractive index detector, and a Waters 478 fluorescence detector (monitored at λ_{exc} = 560 nm and λ_{em} = 575 nm).

For RhB-PDMA, we calculated M_n = 18 900 g mol^{-1} and M_w/M_n = 1.07, and for diblock copolymer RhB-$PDMA_{207}$-*b*-$PDEA_{177}$, we calculated M_n = 43 700 g mol^{-1} and M_w/M_n = 1.08.

Surface Pressure−Area Measurements. Surface pressure−area (π−A) isotherm measurements were carried out on a KSV 5000 Langmuir−Blodgett system (KSV Instruments, Helsinki) installed in a laminar flow hood. Polymer solutions in

(22) Maeda, Y.; Nakamura, T.; Ikeda, I. *Macromolecules* **2002**, *35*, 10172–10177.
(23) Cölfen, H. *Macromol. Rapid Commun.* **2001**, *22*, 219–252.
(24) Kurkuri, M. D.; Nussio, M. R.; Deslandes, A.; Voelcker, N. H. *Langmuir* **2008**, *24*, 4238–4244.
(25) Gaines, G. L., Jr. *Insoluble Monolayers at Liquid-Gas Interfaces*; Interscience: New York, 1966.
(26) Petty, M. *Langmuir-Blodgett Films: An Introduction*; Cambridge University Press: Cambridge, U.K., 1996.
(27) Roberts, G., Ed. *Langmuir-Blodgett Films*; Plenum Press: New York, 1990.
(28) Gonçalves da Silva, A. M. P. S.; Lopes, S. I. C.; Brogueira, P.; Prazeres, T. J. V.; Beija, M.; Martinho, J. M. G. *J. Colloid Interface Sci.* **2008**, *327*, 129–137.
(29) (a) Farinha, J. P. S.; Winnik, M. A.; Hahn, K. G. *Langmuir* **1999**, *15*, 7088. (b) *Langmuir* **2000**, *16*, 3391;(c) Ye, S.; Farinha, J. P. S.; Oh, J. K.; Winnik, M. A.; Wu, C. *Macromolecules* **2003**, *36*, 8749.
(30) Ge, Z.; Cai, Y.; Yin, J.; Zhu, Z.; Rao, J.; Liu, S. *Langmuir* **2007**, *23*, 1114–1122.
(31) (a) Beija, M.; Afonso, C. A. M.; Martinho, J. M. G. *Chem. Soc. Rev.* **2009**, *38*, 2410–2433. (b) Beija, M., PhD Thesis, Universidade Técnica de Lisboa and Université Claude Bernard Lyon 1, 2009.

Chart 1. Molecular Structures of RhB-PDMA and RhB-PDMA$_{207}$-*b*-PDEA$_{177}$

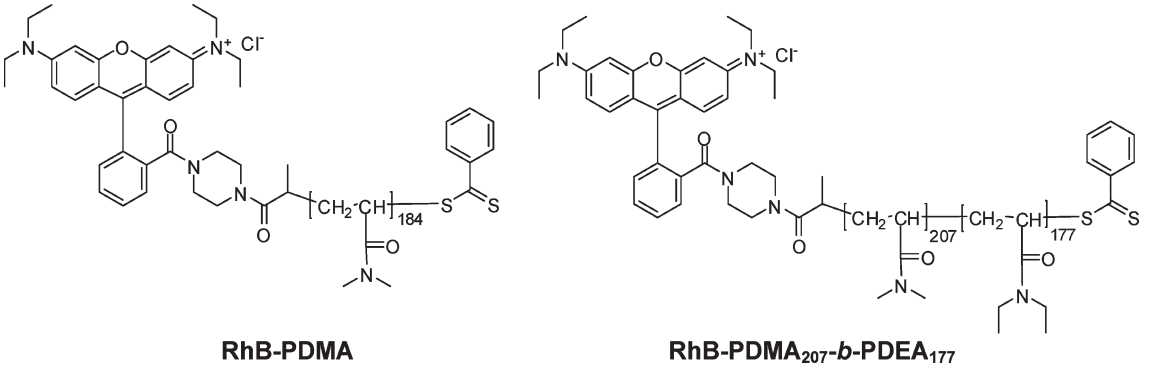

chloroform were prepared with concentrations in the range of 0.5−1.0 mg mL^{-1}. The measurements were started by spreading 50−100 μL of solution. After complete evaporation of the solvent (15 min), the floating layer on the subphase was symmetrically compressed by two mobile barriers at constant speed (5 mm min^{-1}). The temperature of the subphase was maintained by a circulating water bath, and the range of working temperature was 10−40 °C. The $\pi-A$ isotherms did not change with the concentration of spreading solution in the working interval of concentration.

Langmuir−Blodgett Deposition. The spread monolayers at the air−water interface were transferred onto glass substrates by the vertical dipping method. Glass substrates were cleaned by immersion in a chromic/sulfuric acid solution for several minutes, subsequently rinsed and immersed in Milli-Q water, and finally dried in a stream of nitrogen before use. To transfer the film to a single side of the substrate, two substrates were clamped together parallel to the barriers and immersed in the subphase before spreading the polymer solution. After complete evaporation of the solvent, the floating layer was compressed up to the target surface pressure. Following a relaxation period of ~15 min, the deposition was performed at constant surface pressure (3 and 15 mN m^{-1}) with a dipping speed of 2 mm min^{-1}. The transfer ratios were close to unity.

Laser Scanning Confocal Fluorescence Microscopy (LSCFM). Laser scanning confocal fluorescent microscopy (LSCFM) measurements were performed on a Leica TCS SP5 (Leica Mycrosystems CMS GmbH, Mannheim, Germany) inverted microscope (DMI6000) with a 63.3 water-immersion apochromatic objective (1.2 numerical aperture). The 514 nm line of an argon ion laser was used as the excitation light both for imaging and image spectral analysis. The laser intensity was controlled by an acoustic-optical filter system. The fluorescence emission was collected from 530 to 700 nm using the tunable system and beam splitter of the Leica TCS SPC5. The laser power and photomultiplier tube gain were constant for all measurements. The offset was chosen such that the photon counts outside the sample were negligible. The pinhole was always set at 1 Airy unit to discriminate stray light from out-of-focus plans. To ensure that the observed morphology was typical of the film as a whole, a large number of different regions were imaged. The emission spectra were obtained with 10 nm steps and a bandwidth of 10 nm. The data was processed using the Leica Application Suite-Advanced Fluorescence software to obtain the spectra in different regions with a 1 μm diameter in each image.

Atomic Force Microscopy (AFM). The AFM was used in noncontact mode via a Molecular Imaging (model 5100) system using cantilevers with a constant force ranging from 25 to 75 N/m and a resonance frequency of between 200 and 400 kHz.

Results and Discussion

Films at the Air−Water Interface. ***$\pi-A$ Isotherms at 20 °C.*** In Figure 1, we show the $\pi-A$ isotherms of the RhB-PDMA$_{207}$-*b*-PDEA$_{177}$ diblock copolymer (DHBC), homopolymers PDEA and RhB-PDMA, and the theoretical curve of DHBC (crosses) calculated from the homopolymer isotherms weighted by their composition in the copolymer. The experimental curve of DHBC follows the theoretical curve except above the long plateau, where a deviation to larger areas is detected. The trend in the $\pi-A$ curves presented in Figure 1 suggests that the PDEA and RhB-PDMA blocks behave nearly independently at low surface pressure, in agreement with the self-segregation of immiscible PDEA and PDMA blocks at the air−water interface. In the spreading solution, the copolymer exists in the form of a random coil because chloroform is a good solvent for both polymer blocks. Droplets of this solution instantaneously spread at the air−water interface (the spreading coefficient of chloroform on water is positive). Subsequently, as the solvent evaporates at low surface pressures, both PDEA and PDMA hydrophilic polymer blocks adsorb onto the water surface, probably forming distinct domains owing to the differences in affinity with respect to the water subphase (deposition−spreading/evaporation−self-segregation mechanism). Upon compression, the more hydrophilic block (PDMA) desorbs from the interface and immerses into the subphase at nearly constant surface pressure (originating in the long plateau at 6 to 7 mN m^{-1}), promoting a drastic decrease in the area per segment (from 25 to 15 Å^2). Further compression of the PDEA domains that remain at the interface brings about an abrupt increase in surface pressure to 25 to 26 mN m^{-1} when the PDEA blocks start to immerse into the subphase. The covalent bond between the two blocks in DHBC

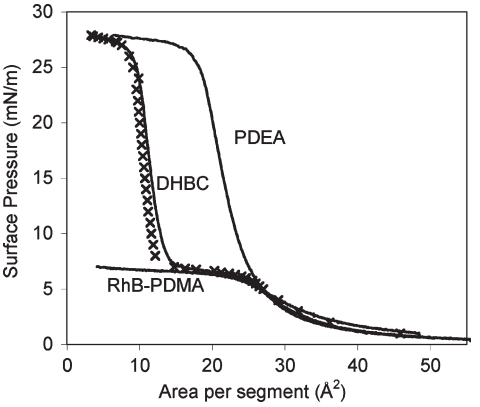

Figure 1. $\pi-A$ isotherm of the RhB-PDMA$_{207}$-*b*-PDEA$_{177}$ diblock copolymer and homopolymers PDEA and RhB-PDMA. The corresponding theoretical curve for the mixture calculated from the $\pi-A$ isotherms of PDEA and RhB-PDMA homopolymers is also shown (×).

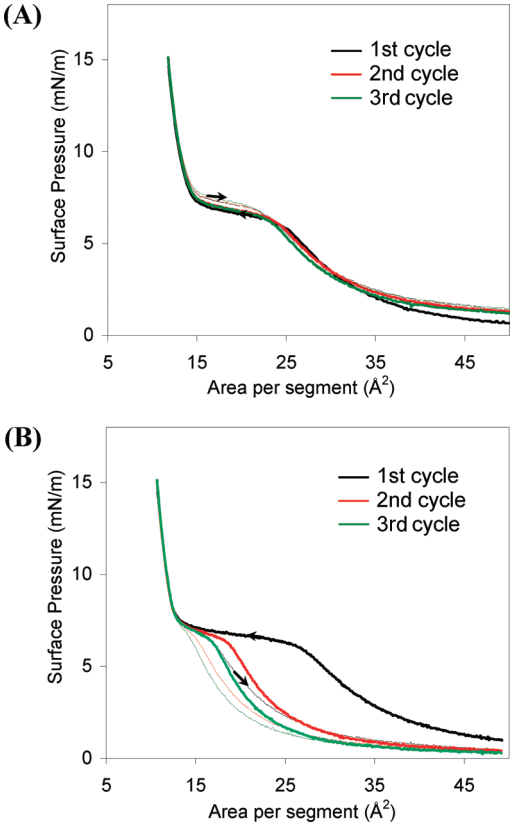

Figure 2. Successive $\pi-A$ compression−expansion cycles for (A) the RhB-PDMA$_{207}$-*b*-PDEA$_{177}$ diblock copolymer and (B) for the mixed PDEA and RhB-PDMA homopolymers, performed at up to 15 mN m^{-1} at 20 °C.

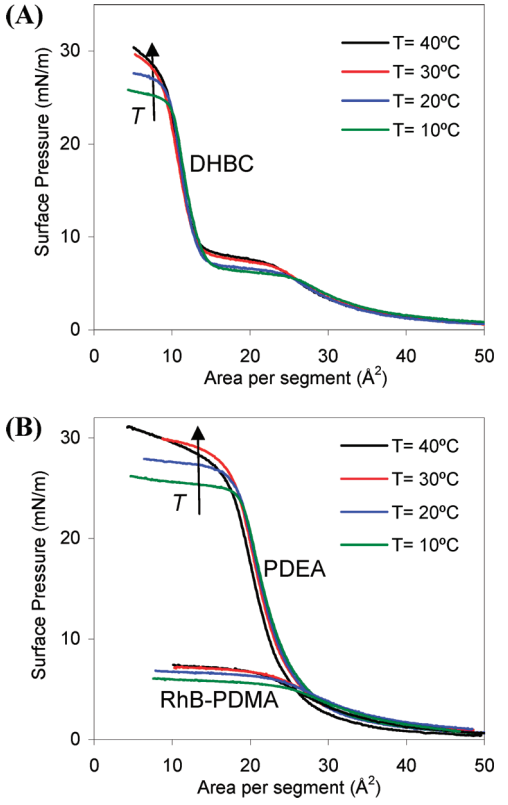

Figure 3. $\pi-A$ isotherms of (A) the RhB-PDMA$_{207}$-*b*-PDEA$_{177}$ diblock copolymer and (B) PDEA and RhB-PDMA homopolymers at the water subphase in the temperature range of 10−40 °C.

hinders the complete immersion of the RhB-PDMA block into the subphase at $\pi < 25$ mN m^{-1} and probably causes the positive deviations shown by the $\pi-A$ isotherm of DHBC at $\pi > 7$ mN m^{-1}.

The experimental $\pi-A$ isotherm of the mixture of homopolymers for the 1:1 (PDEA/PDMA) segmental ratio and the corresponding theoretical curve (×) calculated from the $\pi-A$ isotherms of PDEA and RhB-PDMA homopolymers weighted by their composition in the mixture were also compared with the experimental $\pi-A$ curve of DHBC in Supporting Information, Figure SI.1. The experimental and theoretical curves of mixed homopolymers nearly superimpose, except at low surface pressure where the experimental curve slightly deviates to larger areas per segment. This suggests that in the monolayer regime, before RhB-PDMA immersion, the lateral chain interactions in the mixture are smaller than the lateral average interaction in monolayers of pure homopolymers. The $\pi-A$ isotherm of the mixture clearly presents a longer plateau than the $\pi-A$ isotherm of the DHBC. This indicates that a larger number of RhB-PDMA free chains immerse in the subphase from the mixture of homopolymers than from DHBC because the covalent bond between blocks prevents the irreversible solubilization of the RhB-PDMA block.

Hysteresis. $\pi-A$ successive compression−expansion cycles of the diblock copolymer and the mixture of homopolymers performed at up to 15 mN m^{-1} at 20 °C. The coincidence of the three cycles obtained with the diblock copolymer (Figure 2A) indicates no loss of material into the subphase. However, the compression−expansion cycles are not completely reversible because the expansion plateau is above the compression plateau. This small hysteresis in the plateau region can be ascribed to both the additional hydration of PDMA chains after immersion into the subphase and to steric hindrance.

A different trend was obtained for the mixture of homopolymers (Figure 2B). The successive $\pi-A$ compression isotherms deviate strongly to smaller areas per segment, indicating the progressive loss of PDMA into the subphase. However, the loss is not complete, and the plateau of the second compression isotherm (bold red line) recovers approximately one-third of the first compression plateau (bold black line), which means that a significant amount of PDMA remains at the interface after the first expansion, probably because of interaction or entanglement with PDEA chains.

Effect of Temperature. Figure 3 shows the $\pi-A$ isotherms of the diblock copolymer (A) and the PDEA and PDMA homopolymers (B) at the water subphase in the temperature range of 10−40 °C. The thermoresponsive behavior of the PDEA homopolymer at the air−water interface was previously studied[28] and it was found that the most significant effect on the $\pi-A$ curves is the increase in the plateau surface pressure with the temperature. Although attenuated, the same trend was obtained with the RhB-PDMA homopolymer (B). In the 10−40 °C temperature interval, the RhB-PDMA$_{207}$-*b*-PDEA$_{177}$ diblock copolymer isotherm is close to the weighted sum of the two homopolymer isotherms, as was illustrated for 20 °C (Figure 1). The variation of the $\pi-A$ isotherms of mixed homopolymers with temperature (not shown) is similar to that presented in Figure 3A for the copolymer. This suggests that the PDMA and PDEA blocks in a diblock copolymer or a mixture of these polymers behaves almost independently at the air−water interface, irrespective of temperature.

LB Monolayers. *Effect of Temperature*. Monolayers of the diblock copolymer (D) were transferred at low (3 mN m^{-1}) and high (15 mN m^{-1}) surface pressures and different temperatures

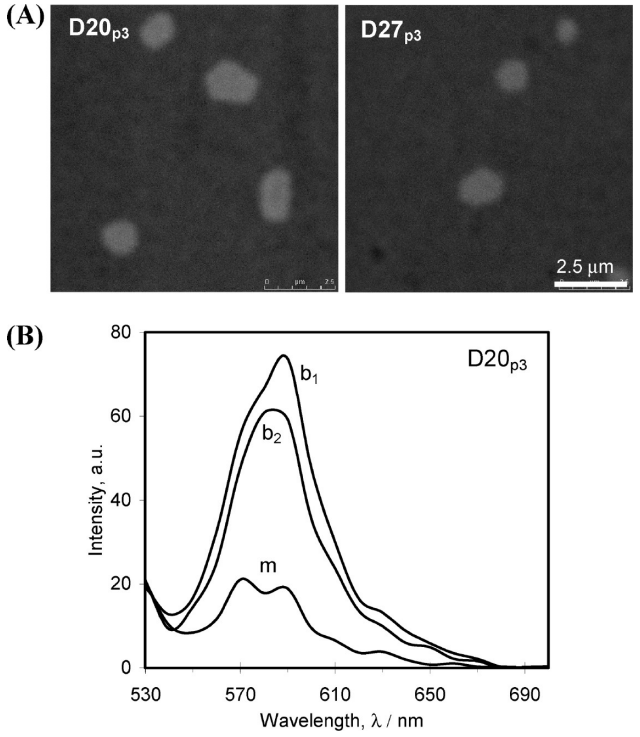

Figure 4. (A) LSCFM images of LB monolayers of the RhB-PDMA$_{207}$-*b*-PDEA$_{177}$ diblock copolymer (D), transferred onto glass substrates at low surface pressure (3 mN m^{-1}) and several temperatures (20 °C (D20$_{p3}$) and 27 °C (D27$_{p3}$)). The image size is $10 \times 10\ \mu m^2$. (B) Fluorescence spectra acquired in 500-nm-radius regions of the D20$_{p3}$ film: bright domains (b_1, b_2) and the matrix (m).

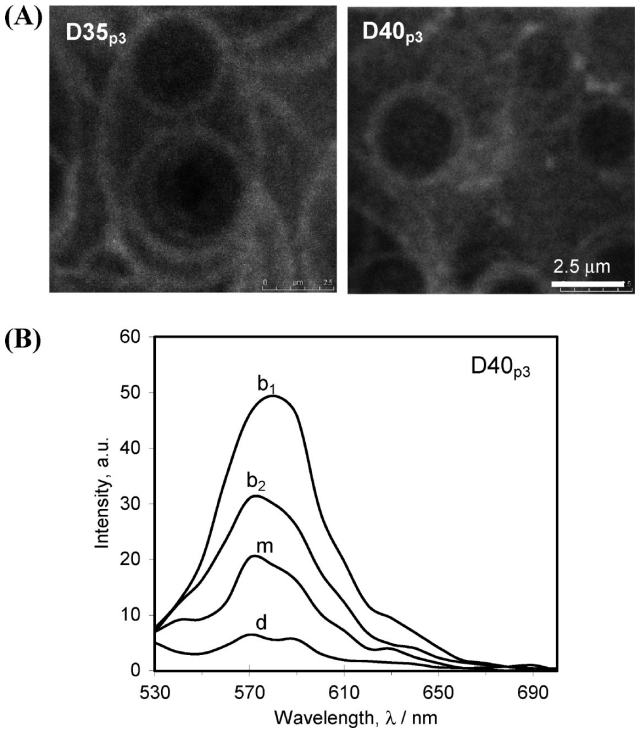

Figure 5. (A) LSCFM images of LB monolayers of the RhB-PDMA$_{207}$-*b*-PDEA$_{177}$ diblock copolymer (D), transferred onto glass substrates at low surface pressure (3 mN m^{-1}) and several temperatures (35 °C (D35$_{p3}$) and 40 °C (D40$_{p3}$)). The image size is $10 \times 10\ \mu m^2$. (B) Fluorescence spectra acquired in several 500-nm-radius regions of the D40$_{p3}$ film: bright domains (b_1, b_2), the matrix (m), and dark domains (d).

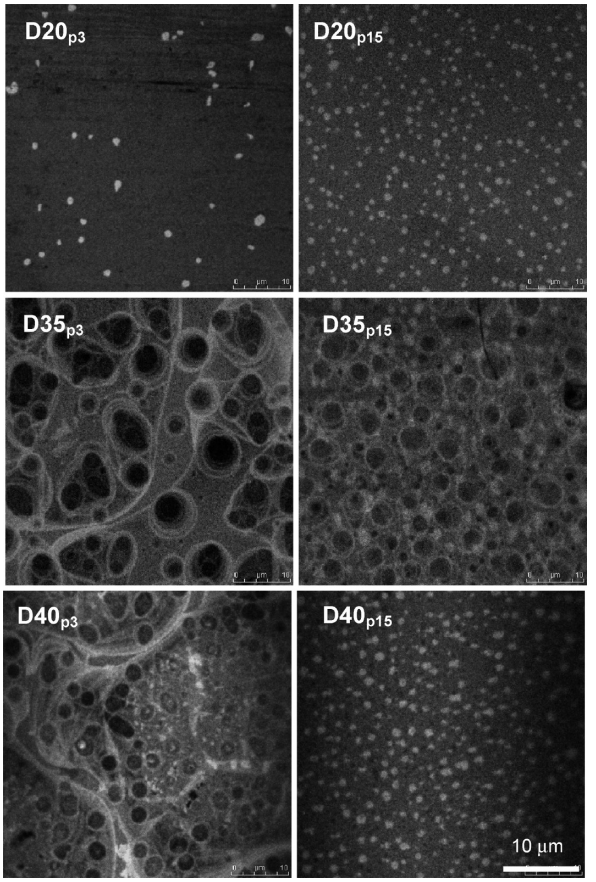

Figure 6. LSCFM images of LB monolayers of RhB-PDMA$_{207}$-*b*-PDEA$_{177}$ transferred at π = 3 mN m^{-1} (first column) and π = 15 mN m^{-1} (second column) at constant temperature: D20$_{p3}$ and D20$_{p15}$ at 20 °C, first row; D35$_{p3}$ and D35$_{p15}$ at 35 °C, second row; D40$_{p3}$ and D40$_{p15}$ at 40 °C, third row. The image size is $50 \times 50\ \mu m^2$.

onto clean glass substrates. Figures 4−6 show LSCFM images of the LB monolayers and the RhB fluorescence spectra acquired in different (1-μm-diameter) regions of the film. Figure 4A shows images of LB monolayers transferred at 3 mN m^{-1} and two different temperatures: 20 °C (D20$_{p3}$) and 27 °C (D27$_{p3}$). The main feature observed at low to room temperature is the appearance of sparse bright microdomains (1 to 2 μm in diameter) dispersed in a less fluorescent matrix.

Fluorescence spectra (Figure 4B) recorded in several (1-μm-diameter) regions of the film show that besides the monomer emission band centered at ca. 570 nm another intense band appears at ca. 590 nm with a shoulder appearing frequently at longer wavelengths (620−640 nm). Rhodamine B is known to form both fluorescent (J-type) and nonfluorescent (H-type) dimers depending on the relative orientation of the dyes.[32,33] Two types of fluorescent (J-type) dimers have been observed: (i) a sandwich-type dimer (d_1) with emission centered at $\lambda_{d_1}^{max}$ = 590 nm, slightly shifted to the red compare to the monomer emission (λ_m^{max} = 570 nm) and (ii) a dimer with oblique geometry (d_2) with the fluorescence around $\lambda_{d_2}^{max}$ = 620 nm shifted to the red compared to that of the sandwich-type (d_1) dimer. The fluorescence spectrum of rhodamine in the matrix (curve m) is essentially composed of the sum of the monomer and the d_1-type emissions with relative intensities varying from one region to the

(32) Kemnitz, K.; Tamai, N.; Yamazaki, I.; Nakashima, N.; Yoshihara, K. *J. Phys. Chem.* **1986**, *90*, 5094–5101.
(33) Yeroshina, S. A.; Ibrayev, N. K.; Kudaibergenov, S. E.; Rullens, F.; Devillers, M.; Laschewsky, A. *Thin Solid Films* **2008**, *516*, 2109–2114.

other. RhB emission is broader and shifted to the red in the bright regions (curves b_1 and b_2), indicating a stronger aggregation of the dyes. The aggregates are essentially formed by d_1-type dimers, with emission centered at 590 nm.

At higher temperature (Figure 5A, $D35_{p3}$ and $D40_{p3}$ at 35 and 40 °C, respectively), the pattern changes drastically into a foamlike complex structure composed of three distinct regions (circular dark domains, bright rings, and a fluorescent matrix). At 35 °C, instead of the isolated bright microdomains observed at low temperature, bright rings form around large dark domains of variable diameter (2−8 μm). These domains are organized in a foamlike structure dispersed in a heterogeneous fluorescent matrix (a superstructure appearing to have fractal morphology). The heterogeneity of the LSCFM images increases with temperature: image $D40_{p3}$ (40 °C) is more heterogeneous than image $D35_{p3}$ (35 °C). This is clear in the large-scale $D40_{p3}$ panel of Figure 6, where the foamlike structure of high contrast coexists with regions of low contrast (brighter regions). In the low-contrast regions, the dark domains become smaller and less dark than those observed in the foam regions and the bright microdomains reappear, with some of them nucleating inside the dark domains.

The RhB fluorescence in the bright regions (curve b_1 in Figure 5B) is composed of both the monomer and the broad emission of d_1, whose contribution seems to dominate. This is probably due to a larger proportion of fluorescent ground-state dimers, but we cannot exclude the dimer fluorescence contribution resulting from the Förster resonance-energy transfer (FRET) from the electronically excited monomers. The energy migration among neighboring RhB molecules enhances the energy transfer to dimers with the consequent decrease in the monomer fluorescence. The electronically excited dimer (d_1) can still fluoresce or transfer energy to a lower-energy dimer (d_2) or other aggregates.[34] The decrease in fluorescence intensity detected in other fluorescent regions (curve b_2) is associated with an increase in monomer emission, which is certainly caused by a different organization of the dyes with larger average dye-to-dye distances. The fluorescence emission observed in the dark regions (curve d), where RhB dyes are more separated, is composed of monomer and dimer emissions resembling the spectra observed in the fluorescent matrix at low temperatures, where the monomer contribution is significant (Figure 4B, curve m). The spectrum collected in the matrix (curve m) seems to be in between those recorded in the bright and dark regions.

The images shown in Figures 4A and 5A reveal the schizophrenic behavior of the RhB-$PDMA_{207}$-*b*-$PDEA_{177}$ diblock copolymer with temperature. At low temperature, (Figure 4A) the RhB-PDMA block dominates the interior of the fluorescent microdomains (RhB-PDMA-core aggregates), switching to the outside for films deposited at temperatures above the LCST of PDEA (Figure 5A), with the interior becoming richer in PDEA (PDEA-core aggregates).

Below the LCST of PDEA (~32 °C), both the PDEA and PDMA blocks are hydrophilic. Despite the chemical and structural similarities between PDEA and PDMA, the $\pi-A$ isotherms indicate distinct affinities of these homopolymers for the water subphase (Figure 1). In the low-pressure regime ($\pi < 6$ mN m^{-1}), both blocks adsorb at the interface and the LB films transferred onto hydrophilic substrates at 3 mN m^{-1} reproduce the monolayer structure of the diblock copolymer at the air−water interface. Because the PDMA block is end labeled with rhodamine, the bright fluorescent microdomains reveal PDMA-rich domains. Rhodamine dye has a high tendency to aggregate in solution (water, methanol, and ethanol) and when incorporated into solid-state matrixes and LB films.[32−35] The rhodamine aggregates can already be present in the spreading solution and/or formed during the encounter of dye-labeled polymer chain ends during chloroform evaporation after spreading. The rhodamine aggregates are present in both the matrix and in bright domains (Figure 4B). The fluorescence of the matrix suggests the partial miscibility of PDEA and PDMA at the air−water interface whereas the sparse bright microdomains indicate a high density of rhodamine mostly forming dimers and eventually higher-order aggregates. However, the apparent homogeneity of the matrix, observed on the LSCFM images, can occult microheterogeneities compatible with partial miscibility that are visible only at higher spatial resolution.

At $T \geq 32$ °C, the thermoresponsive PDEA block becomes hydrophobic but the PDMA block remains hydrophilic. Consequently, the PDEA blocks self-aggregate, forming dark domains of PDEA surrounded by a bright fluorescent ring of RhB-PDMA (Figure 5). Therefore, we believe that at $T < 32$ °C the PDMA-core domains are induced by the self-aggregation of rhodamine whereas at $T \geq 32$ °C it is the hydrophobicity of PDEA that determines the new morphology.

Most of the dark domains in image $D35_{p3}$ present diameters much larger than the length of two single chains of the RhB-$PDMA_{207}$-*b*-$PDEA_{177}$ diblock in its extended conformation. (The theoretical length of one fully extended chain is around 102 nm.) This implies that most of the dark domains must also include the dye (Figure 5B, curve d). In fact, a deeper analysis of the large, dark domains reveals smaller domains surrounded by fluorescent rings with a self-similar morphology typical of a fractal structure. This is clear in Figure SI.2, which is an amplification of a small area of image $D35_{p3}$ in Figure 6. The fluorescence intensity can be lowered at high temperature owing to the percentage increase in rhodamine nonfluorescent H dimers with respect to fluorescent J dimers.[36]

At 40 °C, the dark domains become smaller and the bright microdomains reappear (bottom image $D40_{p3}$ in Figure 6). This indicates that the self-segregation of PDEA induced by increasing temperature, bringing together the covalently bounded RhB-PDMA blocks, favors rhodamine aggregation and the consequent reappearance of the bright fluorescent domains. However, the spectra are broader in $D40_{p3}$ (Figure 5B) than in $D20_{p3}$ (Figure 4B), owing to a larger contribution of the monomer emission at 40 °C. This indicates a change in dye organization induced by the core−shell inversion.

Effect of Surface Pressure. Figure 6 shows LB monolayers transferred at $\pi = 3$ mN m^{-1} (left column) and $\pi = 15$ mN m^{-1} (right column) at several temperatures. At 20 °C (top row), the shape and size of the very bright microdomains are nearly invariant with surface pressure, but the number density increases drastically in the film transferred above the plateau of the $\pi-A$ isotherm ($D20_{p15}$) when compared to that observed at low pressure ($D20_{p3}$). In fact, the domain density increases much more than the estimated (3:1) area reduction from the monolayer compression. This means that the number of microdomains increases with the surface pressure increase (i.e., new domains appear during the compression of the monolayer).

(34) Arbeloa, F. L.; Ojeda, P. R.; Arbeloa, I. L. *J. Chem. Soc., Faraday Trans. 2* **1988**, *84*, 1903–1912.

(35) Malfatti, L.; Kodchob, T.; Aiello; Daniela; Testa, R.; Innocenzi, P. *J. Phys. Chem.C* **2008**, *112*, 16225–16230.

(36) Vuorimaa, E.; Ikonen, M.; Lemmetyinen, H. *Chem. Phys.* **1994**, *188*, 289–302.

In the low-pressure regime (below the first plateau), both the PDEA and RhB-PDMA blocks adsorb at the interface. Upon compression to the plateau regime, RhB-PDMA (covalently bound to the PDEA block) immerses into the subphase, adopting a mushroom-like conformation. Consequently, the morphology and thickness of the LB films transferred onto the hydrophilic glass substrate at surface pressures above the plateau should reflect the different distribution of chains at the air−water interface. Such an arrangement of blocks at the interface is responsible for LB films with double-layer structure: the RhB-PDMA-rich layer is in contact with the hydrophilic substrate whereas the PDEA-rich layer stays above the substrate. This distribution is supported by the preliminary AFM image of the $D20_{p15}$ LB film (Figure SI.3). This structure favors rhodamine interaction in the PDMA-rich layer, resulting in the density increase for bright microdomains.

At 35 °C and surface pressure above the plateau ($D35_{p15}$), the diameter of dark domains is reduced, promoting the formation of bright microdomains (absent at low pressures) in the exterior of the dark domains. As described before, when the film is transferred the rhodamine-rich microdomains formed in the immersed hydrophilic layer of RhB-PDMA are deposited directly onto the substrate, underneath the PDEA-rich layer. The dark domains in image $D35_{p15}$ are smaller than the dark domains in $D35_{p3}$ as a consequence of the decrease in area resulting from compression. Simultaneously, the contrast between the dark interior and the bright exterior of the domains is lower for higher pressure because of the higher density of rhodamine in the film.

At 40 °C, the film structure strongly depends on the deposition pressure. The images of films deposited at 3 mN m^{-1} ($D40_{p3}$) show a complex fractal-like foam structure, and the films deposited at 15 mN m^{-1} ($D40_{p15}$) show a dense distribution of very bright microdomains in a nearly homogeneous fluorescent matrix. Two factors might contribute to the absence of dark domains in image $D40_{p15}$. First, the reduction in surface area due to compression probably induces the formation of dark domains with sizes that are less than the spatial resolution of LSCFM. Second, in the double-layer structure of the LB film, the dark domains might become undetectable because of the brightness of the microdomains formed in the RhB-PDMA-rich layer underneath. The appearance of a double-layer structure in LB films transferred at surface pressures above the plateau ($D20_{p15}$, $D35_{p15}$, and $D40_{p15}$) can be explained by two factors: (i) the hydrophobic aggregates formed at pressures below the plateau form the top layer; and (ii) the RhB-PDMA chains immersed at the plateau surface pressure assemble to form the layer in contact with the substrate.

The patterns observed in LB films formed at low pressures (3 mN m^{-1}) in the monolayer regime depend on the deposition temperature (Figure 6, left column), and the patterns observed in films deposited at 15 mN m^{-1} (above the plateau surface pressure) are quite similar at 20 and 40 °C (Figure 6, right column). At 20 °C, the patterns that result at both low and high surface pressures are formed by the bright microdomains of RhB-PDMA distributed in a fluorescent matrix. At 35 °C, dark domains surrounded by bright rings are formed at low pressures and coexist with the bright microdomains resulting from the immersion of RhB-PDMA in the subphase occurring at the plateau surface pressure. Finally, at 40 °C, the small, dark domains resulting from the hydrophobic aggregates are formed at pressures below the plateau ($D40_{p3}$). The changes observed by increasing the temperature from 35 to 40 °C can be explained by a synergetic effect. Above the LCST, the increase in temperature increases the thermoaggregation of PDEA that

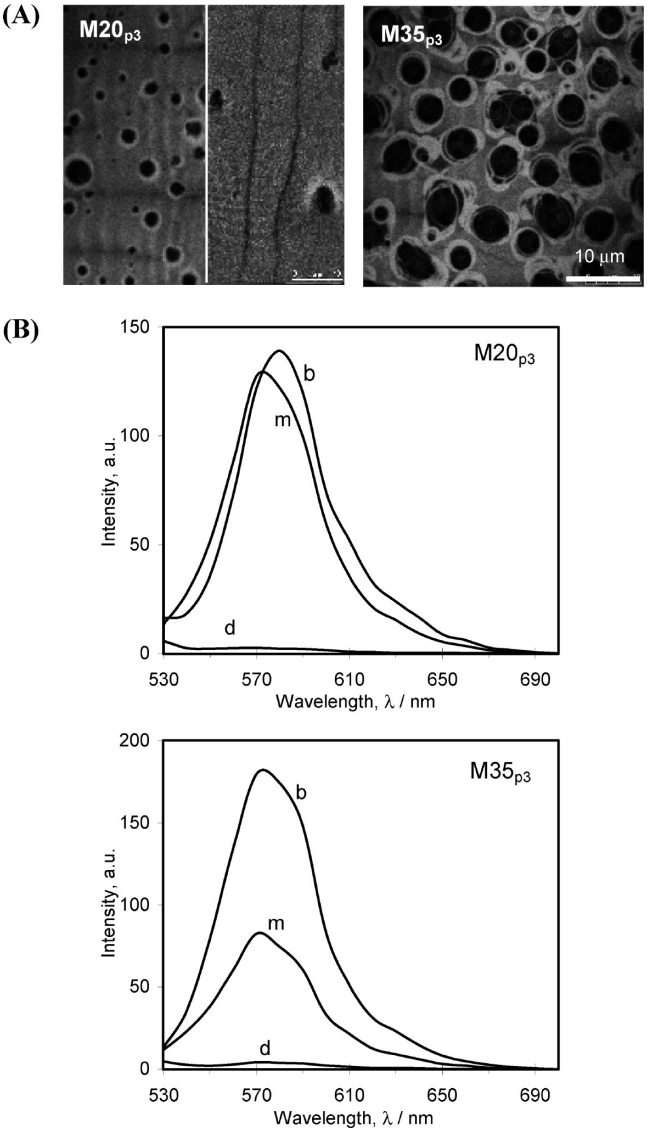

Figure 7. (A) LSCFM images of LB monolayers of the mixture of homopolymers (M) transferred onto glass substrates at low surface pressure (3 mN m^{-1}) and several temperatures (20 °C ($M20_{p3}$) and 35 °C ($M35_{p3}$)). Image size 50 × 50 μm^2. (B) Fluorescence spectra acquired in several 500-nm-radius regions of films $M20_{p3}$ and $M35_{p3}$: bright domains (b), the matrix (m), and dark domains (d).

simultaneously drags together the RhB-PDMA blocks. This enhances the nucleation and fusion of bright domains, which in turn mask the small, dark domains of the top layer.

Mixture of Homopolymers. Figure 7A shows confocal images of mixed homopolymers (M) with a 1:1 segmental ratio transferred onto glass substrates at a low surface pressure (3 mN m^{-1}) at 20 °C ($M20_{p3}$) and 35 °C ($M35_{p3}$).

At 20 °C, two distinct patterns were observed: the left image, $M20_{p3}$, in Figure 7A displays circular dark domains of variable size dispersed in a bright fluorescent matrix; the right image in the same Figure presents dark domains of different shapes, from nearly circular to long stripes, in a heterogeneous matrix. These patterns appear in different regions of the film. The two patterns arise from the organization of the polymers in three coexisting phases: circular or striped dark domains of the less-hydrophilic, unlabeled component PDEA; bright rings of RhB-PDMA surrounding the circular dark domains; and the fluorescent background resulting from the partial miscibility of these homopolymers

at the air−water interface. The spreading of the homogeneous solution of the homopolymers in chloroform leaves a mixture of polymers at the air−water interface, stabilized by hydrogen bonding with the water subphase. The diffusion of these polymer chains in the two dimensions of the monolayer is restricted, preventing the complete phase separation expected by the unfavorable enthalpy and small entropy of mixing.

Temperature increasing to 35 °C ($M35_{p3}$) favors the phase separation of the polymers: the dark domains and the bright rings increase in size whereas the area of the weakly fluorescent background decreases. The high contrast between dark domains and bright rings is associated with the presence of pure PDEA and RhB-PDMA phases in the mixture, confirming the lower miscibility of PDEA and RhB-PDMA in the homopolymer mixture. At 40 °C, the general pattern of the image becomes more heterogeneous and complex. Dark domains prevail in some regions but the bright domains associate in other regions, suggesting that phase separation increases with temperature as a result of the increase in PDEA hydrophobicity.

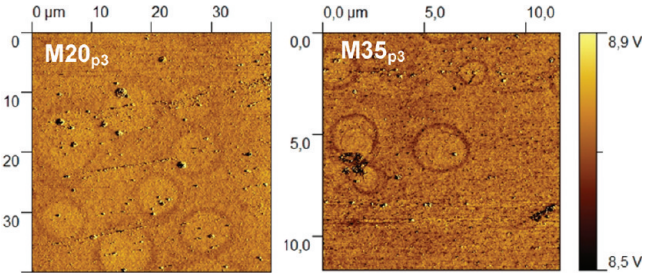

Figure 8. AFM phase images of the LB monolayer of the mixture of PDEA and RhB-PDMA homopolymers transferred onto glass at 3 mN m^{-1} and two temperatures (20 °C ($M20_{p3}$) and 35 °C ($M35_{p3}$)). These images do not illustrate the increase in ring diameter with temperature because the short scale of $M35_{p3}$ shows only the small domains.

The RhB fluorescence spectra of the mixtures (Figure 7B) in the fluorescent regions at low temperature (20 °C, $M20_{p3}$) show a higher contribution of d_1 dimers in the bright regions (curve b) than in the matrix (curve m), in accordance with the corresponding spectra of the block copolymer ($D20_{p3}$, Figure 4B). The fluorescence spectra of the mixtures at 35 °C ($M35_{p3}$) show that despite the difference in intensity the shapes of the spectra (curves b and m) are identical. The spectra of bright domains at 35 °C have a larger contribution of monomers to dimers than at 20 °C, probably resulting from a conversion of fluorescent to nonfluorescent dimers with increasing temperature.[36]

The $M20_{p3}$ image of the mixture (Figure 7A) and the corresponding $D20_{p3}$ image of the diblock copolymer (Figures 4A and 6) are substantially different: the bright microdomains of $D20_{p3}$ were not observed in the mixtures of homopolymers whereas the dark domains in $M20_{p3}$ were not observed in $D20_{p3}$. A common feature is the fluorescent matrix that results from PDEA and PDMA mixing. The absence of dark domains in $D20_{p3}$ indicates a higher miscibility of PDEA and PDMA in the diblock copolymer than in the homopolymer mixture in $M20_{p3}$. However, we cannot exclude the existence of very small PDEA domains (dark domains) in the copolymer film that cannot be resolved by the confocal microscope. Furthermore, the high density of rhodamine in the bright rings surrounding the PDEA dark domains of

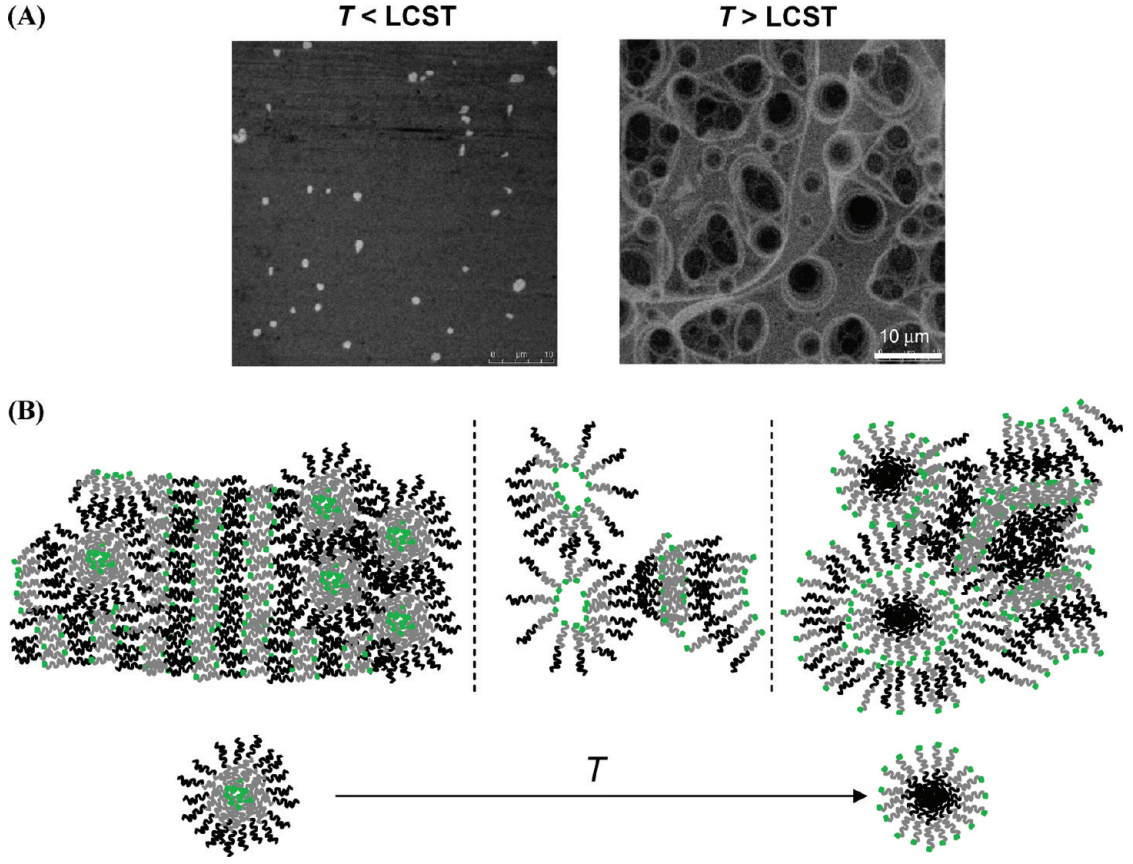

Figure 9. (A) LSCFM images at T < LCST and at T > LCST illustrating the core−shell inversion by temperature increase (schizophrenic behavior of DHBC). (B) Schemes of conformational changes of the RhB-$PDMA_{207}$-*b*-$PDEA_{177}$ diblock copolymer. PDEA block (black), PDMA block (gray), and rhodamine (green).

$M20_{p3}$ indicates the preferential location of the dye in the vicinity of the ethyl groups of PDEA. The absence of large dark domains in the copolymer film at low temperatures is attributed to the block connectivity that favors rhodamine aggregation instead of the interaction with the hydrophobic groups of PDEA. Indeed, the tendency of rhodamine to aggregate to form d_1 dimers leads to the formation of a few very bright regions in the PDMA-rich domains dispersed in a weakly fluorescent matrix (Figure 4B).

Confocal images of the mixed homopolymers transferred at a pressure above the plateau (15 mN m^{-1}) show bright microdomains in a dark matrix. (Figure SI.4 shows image $D20_{p15}$ at 20 °C; similar images were obtained at 35 and 40 °C.) This observation indicates that a significant portion of the RhB-PDMA homopolymer is retained in the film at high surface pressure, above the plateau, possibly anchored by chain entanglement and/or rhodamine aggregates. This is in agreement with the results obtained in successive compression−expansion cycles (cf. Figure 2).

Finally, in Figure 8, we show AFM phase images of LB monolayers of mixed homopolymers transferred at 3 mN m^{-1} and several temperatures (20 °C ($M20_{P3}$) and 35 °C ($M35_{p3}$)). The foam structure was detected only in phase mode, indicating that the film height is nearly homogeneous or that the small height variations involved cannot be detected with these substrates. The film structure is composed of rings of RhB-PDMA enclosing the more hydrophobic PDEA domains. The lower elasticity of the rings of RhB-PDMA, owing to the rhodamine interaction, was detected in AFM phase-mode scans. However, the peculiar foam pattern observed in the LSCFM images of DHBC above the LCST of PDEA was not detected in topographic or phase AFM modes. This is probably because the covalent bond between the two blocks inhibits the phase separation of PDEA and PDMA, inducing the formation of domains of undistinguishable elasticity in AFM phase images.

Concluding Remarks

The analysis of the $\pi-A$ isotherms suggests that PDEA and PDMA behave almost independently at the air−water interface either when covalently bonded in the DHBC or as a mixture of homopolymers. However, LSCFM images of LB monolayers transferred at several temperatures give new insight into the thermoresponsive behavior of the DHBC, revealing an unexpected core−shell inversion of the film structure (Figure 9A). At temperatures below the LCST of PDEA, bright RhB-PDMA-rich (core) microdomains formed, probably because of the tendency of rhodamine to aggregate.[32] At temperatures above the LCST of PDEA, DHBC organizes with PDEA chains in the center of (dark-core) domains, surrounded by bright rings of RhB-PDMA. This indicates that when the temperature is increased above the LCST of PDEA the self-segregation of the thermoresponsive block into the hydrophobic globule (PDEA-core) forces the RhB-PDMA chains to organize around the PDEA dark cores, forming bright rings.

In Figure 9B, we show 2D schemes illustrating the variation of the DHBC organization with temperature. At low temperature (left), both blocks are hydrophilic and spread at the air−water interface; the bright core domains result from a high density of rhodamine aggregates. Increasing temperature (middle) promotes conformational changes or a reorientation of the chains. Above its LCST (right), PDEA becomes hydrophobic and consequently self-aggregates into dense cores (2D globules). It is worth noting that at low temperature (left) the parallel alignment of the PDEA blocks leads to the formation of dark parallel stripes besides the bright microdomains (green cores). In fact, the stripe pattern was not detected in the DHBC films ($D20_{p3}$) probably because of the miscibility of the two blocks at the interface for $T <$ LCST. However, the stripe pattern was observed in a few samples of mixed homopolymers at 20 °C ($M20_{P3}$ in Figure 7A). The foam-like superstructure displayed by diblock copolymer RhB-$PDMA_{207}$-*b*-$PDEA_{177}$ at $T >$ LCST suggests the potential applicability of this DHBC as a novel surfactant.[23]

For the homopolymer mixture, the free chains of PDEA are able to self-segregate into wider dark domains observable by LSCFM, but the core−shell inversion due to increasing temperature does not occur. The bright domains observed in the copolymers at 20 °C ($D20_{p3}$) are due to the aggregation of rhodamine. These domains, not observed in the mixture of homopolymers ($M20_{p3}$ and $M35_{p3}$), are partially destroyed by increasing temperature and polymer segregation above the LCST of PDEA ($D35_{p3}$).

From the above discussion, we conclude that the schizophrenic behavior of DHBC results from the synergism of the thermoresponsive behavior of PDEA, the aggregation of rhodamine at the end of PDMA chains, and the covalent bonding between blocks.

Acknowledgment. CQE, CQFM, and IN-Institute of Nanosciences and Nanotechnlogy acknowledge financial support from the Fundação para a Ciência e a Tecnologia (FCT) and FEDER (POCI/QUI/61045/2004 and POCI/CTM/56382/2004). We are indebted to Dr. Quirina Ferreira for the availability and assistance in AFM experimental execution. R.I.S.R. and M.B. thank the FCT for grants SFRH/BD/41326/2007 and SFRH/BD/18562/2004, respectively.

Supporting Information Available: Surface pressure−area isotherms of the homopolymer mixture, successive $\pi-A$ compression−expansion cycles for DHBC, LSCFM image of the LB monolayers of DHBC, an amplification of image $D35_{p3}$ in Figure 6, AFM image of $D20_{p15}$, and an LSCFM image of the LB monolayer of the mixture of homopolymers transferred at 20 °C and 15 mN m^{-1} ($M20_{p15}$). This material is available free of charge via the Internet at http://pubs.acs.org.